Korean J. Chem. Eng., 33(2), 711-719 (2016)
DOI: 10.1007/s11814-015-0186-8

pISSN: 0256-1115
eISSN: 1975-7220

Synthesis and characterization of a new polymeric surfactant for chemical enhanced oil recovery

Keshak Babu[**], Nilanjan Pal[*], Vinod Kumar Saxena[**], and Ajay Mandal[*,†]**

*Department of Petroleum Engineering, Indian School of Mines, Dhanbad 826 004, India
**Department of Chemical Engineering, Indian School of Mines, Dhanbad 826 004, India
(*Received 30 April 2015 • accepted 28 August 2015*)

Abstract−Chemical enhanced oil recovery methods are field proven techniques that improve efficiency and effectiveness of oil recovery. We have synthesized polymeric surfactant from vegetable oil (castor oil) for application in chemical enhanced oil recovery. First, an eco-friendly surfactant, sodium methyl ester sulfonate (SMES) was synthesized from castor oil, and then the polymeric surfactant (PMES) was produced by graft co-polymerization reaction using different surfactant to acrylamide ratios. The synthesized PMES was characterized by FTIR, FE-SEM, EDX, TGA, DLS analysis. The performance of PMES as a chemical agent for enhanced oil recovery was studied by measuring the interfacial tension (IFT) between crude oil and PMES solution, rheological behavior and contact angle against sandstone surface. Addition of sodium chloride in PMES solution reduced the IFT to an ultra-low value (2.0×10^{-3} mN/m). Core flooding experiments were conducted in sandpack system, and 26.5%, 27.8% and 29.1% additional recovery of original oil in place (OOIP) was obtained for 0.5, 0.6 and 0.7 mass% of PMES solutions, respectively, after conventional water flooding.

Keywords: Polymeric Ssurfactant, Synthesis, Interfacial Tension, Contact Angle, Enhanced Oil Recovery

INTRODUCTION

Chemical enhanced oil recovery (EOR) processes encompass a variety of mechanisms, including use of polymer to increase the macroscopic efficiency by improving the mobility control [1-3], a reduction in the oil-water interfacial tension [4-6] and wettability alteration [7]. The most widely used chemical method for enhanced oil recovery is polymer flooding. The basic idea behind using water-soluble polymers in many oil fields' operation and various enhanced oil recovery processes is to reduce the mobility of the displacing phase and, consequently, to improve the sweep efficiency [8]. High molecular weight water soluble polymers at low concentrations increase viscosity of water significantly. Additionally, polymer adsorption decreases the permeability to water, which also reduces the mobility [9]. There are many water-soluble polymers with potential use in these applications. Surfactants are considered as good enhanced oil recovery agents since 1970s because they can significantly lower the interfacial tension and alter wetting properties [10]. Displacement by surfactant solutions is one of the important tertiary recovery processes by chemical solutions [5,11]. The addition of surfactant decreases the interfacial tension between crude oil and formation water, lowers the capillary forces, facilitates oil mobilization, and enhances oil recovery. In surfactant polymer (SP) flooding for enhanced oil recovery, surfactant and polymer solutions are injected with the objectives to reduce IFT between crude oil and water and increase the viscosity of the displacing fluid. However, use of both surfactant and polymer is cost effective and proper formulation and design is also very much complicated, and there may be undesirable phase separation due to improper mixing. Recently, some interesting works have been reported on synthesis of polymeric surfactants for its application in enhanced oil recovery [12,13]. The main advantages of polymeric surfactant is that it has the ability to improve the mobility ratio and reduction of interfacial tension. Thus, injection of only one chemical is sufficient for significant enhanced oil recovery.

There is increasing interest in the synthesis of tailor-made polymeric surfactants. Although necessarily less well-defined than small molecule surfactants, polymeric surfactant probably offers greater opportunity in terms of its flexibility, diversity and functionality [14]. The basic idea to synthesize the polymeric surfactants is to attach different functional groups of polymer to a hydrophobic group of a surface active monomer under standard methods in presence of an initiator. Cao and Li [13] synthesized a novel series of polymeric surfactants based on carboxy methyl cellulose and alkyl poly(etheroxy) acrylate with an IFT value of about 1 mN/m. Ye et al. [15] reported synthesis of a new polymeric methyl ester sulfonate (PMES) via a polymerization process. The purpose of this process is to graft the sulfonated group to the hydrophobic groups of the polymer backbone. Xu et al. [16] synthesized a new kind of polymeric surfactant, acrylamide-alkyl (phenyl) poly (oxyethylene) acrylate copolymer, which has surface tension of 25-32 mN/m and interfacial tension of about $5\text{-}10^{-1}$ mN/m. Elraies et al. [12] synthesized a polymeric surfactant by attaching different sulfonate groups of sodium methyl ester sulfonate to a hydrophobic group of acrylamide monomer. Thereby, polymeric surfactants can be used as replacement in mixtures of polymers and conventional surfactants in many fields for EOR.

Our aim was to synthesize and characterize a new polymeric

†To whom correspondence should be addressed.
E-mail: mandal_ajay@hotmail.com

surfactant for its application in enhanced oil recovery. To reduce the cost of polymeric surfactant production, much attention is focused towards agriculturally derived nonedible oil as alternative feed stocks for petroleum industries. The polymerization was conducted with an excess of surfactant to acrylamide ratio for interfacial tension reduction and viscosity control. The surfactant used in this study was synthesized by using ricinoleic acid methyl ester present in castor oil. The synthesized polymeric surfactant was characterized by FTIR, FE-SEM, EDX, TGA analysis. The suitability of the polymeric surfactant as chemical flooding agent was then studied by measuring their rheological behavior and interfacial properties in aqueous solution and wettability alteration. Finally, a series of flooding experiments were conducted to evaluate the performance of the polymeric surfactant for enhanced oil recovery.

MATERIALS AND METHODS

1. Materials

Sodium methyl ester sulfonate (SMES) synthesized from castor oil was used as a surfactant in the polymerization. Potassium persulfate (99%), acrylamide (≥99%) and acetone were purchased from Merck India. Sodium chloride 99% (Loba Chemie) in powder form was used to vary the salinity of the aqueous solutions. The crude oil used in IFT measurement and in the flooding experiments was collected from Ahmedabad oil-field (India). The oil has total acid number of 0.038 mg KOH/g, gravity of 38.86 °API and viscosity of 11.9 Pa·s at 30 °C.

2. Synthesis of Polymeric Methyl Ester Sulfonate

First, methyl ester sulfonate was synthesized from castor oil by sulfonation method [17]. The main component of castor oil is hydrogenated form of fatty acid known as ricinoleic acid methyl ester (RAME) (85-90%). The details are given in our earlier paper. The schematic representation of proposed chemical reaction for the formation of SMES surfactant has been depicted in Fig. 1(a).

Polymerization was conducted using above mentioned sodium methyl ester sulfonate (SMES) as the surfactant, acrylamide as monomer (AAM) with potassium persulfate (KPS) as an initiator. The composition of the polymeric surfactant was taken at different weight ratios of SMES : AAM (1 : 0.4, 1 : 0.5, 1 : 0.6, 1 : 0.8 and 1 : 1). The corresponding products were designated as P1, P2, P3, P4 and P5. The surfactant solution was prepared by dissolving appropriate amount of SMES in 80 mL distilled water in three-neck round bottom flask. An appropriate amount of acrylamide monomer was dissolved in 10 mL distilled water in a beaker. Afterwards, the acrylamide solution was added to the surfactant solution and stirred under nitrogen atmosphere until a clear solution was observed. The solution was heated at 65 °C, and the initiator (KPS) was added dropwise by using injection glass syringe. Then, the polymerization was conducted for 2 hours using an auto shaker oil bath. During the polymerization reaction the flow rate of nitrogen was properly controlled due to viscous nature of crude product. The crude product was then extracted with acetone and dried at 60 °C in an oven for 12 hours. The schematic representation of proposed chemical reaction for synthesized polymeric surfactant (PMES) has been depicted in Fig. 1(b) [18-21]. During free radical polymerization, the active radical site is generated by the presence of radical initiator.

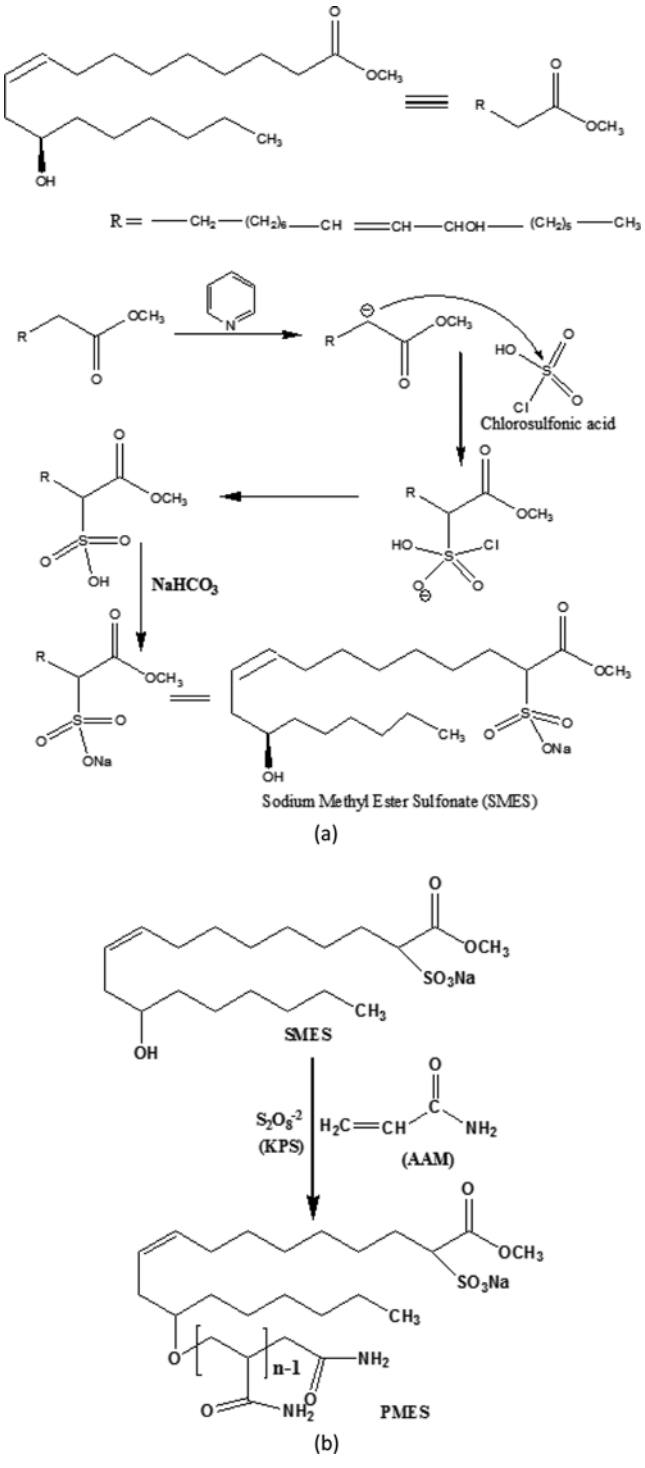

Fig. 1. Schematic representation of proposed chemical reaction for synthesis of (a) SMES and (b) PMES.

In the above surfactant (SMES) there are two probabilities to generate the free radical into the surfactant chain. Either break-down of the -OH bond or cleavage of C=C (unsaturation) bond. Since the polarity of the -OH bond is higher than C=C bond, this results in a higher proportion of free radical for grafting on -OH site without splitting of C-C unsaturation bond. As a matter of fact, the formation of polyacrylamide chain took place onto the hydroxyl sub-

stituent (-OH) of surfactant (SMES) rather than unsaturation portion of the surfactant. This is also supported by the presence of ether group in FTIR. The molecular weights have been evaluated from intrinsic viscosity data of different polymeric surfactants using the Mark-Houwink equation [22,23]. The molecular weights of different polymeric surfactants P1, P2, P3, P4 and P5 were 2.465382×10^6, 3.695453×10^6, 4.598701×10^6, 5.502811×10^6 and 6.222049×10^6 g/mol, respectively.

3. Analysis of FTIR

The synthesized PMES was milled with potassium bromide (KBr) to form a fine powder. This powder was then compressed into a thin pallet for FTIR analysis. The FTIR spectrophotometer (Perkin Elmer-Spectrum Two) was used to determine the chemical functional group present in the synthesized PMES. The graphs were generated using Fourier transform infrared spectroscopy and infrared spectrum lies between 4,000 and 400 cm^{-1}.

4. Thermal Stability Analysis

The thermo-gravimetric analysis of the polymeric surfactant was obtained using a TGA instrument Netzsch-STA 449 Jupiter. High resolution TGA operating at ramp 23.7 °C/min with resolution 6.0 °C from 25 °C to 500 °C in a high purity flowing nitrogen atmosphere. Approximately 0.04 g of finely ground sample was heated in an open platinum crucible. The TGA determines changes of weight loss of the polymeric surfactant (PMES) against temperature.

5. FE-SEM and EDX Analysis

The surface morphology of the prepared polymeric surfactant was examined by FE-SEM SUPRA 55 ZEISS (Germany). The PMES was conditioned in a vacuum oven at 60 °C for 24 h for moisture reduction and coated with platinum prior to analysis to get more accurate results. Small amount of dried powders (0.01 g) were placed on sticky carbon tape on standard Al mounts. The charging of samples due to presence of water was mitigated with the platinum coating and viewed at 20 kV.

Elemental analysis of the polymeric surfactant was recorded using SUPRA 55 ZEISS (Germany). The polymeric surfactant was sputtered with gold. Energy dispersive X-ray spectroscopy (EDX) spectrum of the energy versus relative counts of the detected X-Ray was obtained and evaluated for qualitative and quantitative determinations of the elements in polymeric surfactant.

6. Measurement of Dynamic Light Scattering (DLS)

The particle size analysis of PMES surfactant in aqueous solution was determined with a ZETASIZER (Nano- S90, Nano series Malvern) at 30±0.1 °C. The laser wavelength was 633 nm and the scattering angle, 90°. The refractive index (1.332) of each solution was measured with a portable refractrometer (refracto 30PX mettler). All samples were prepared in distilled water and filtered using a 0.2 μm pore size membrane to remove possible dust particles from the solution. The absorbance of PMES solutions was measured by using UV-1800 (UV-VIS spectrophotometer Shimadzu, Japan) at wavelength of 217 nm. The value of absorbance obtained was 2.33.

7. Measurement of Interfacial Tension (IFT)

Interfacial tension between different polymeric surfactant solutions and crude oil was measured by spinning drop method. Model SVT 15 spinning drop tensiometer equipped with video camera was used to determine the IFT at 29 °C. For each sample, IFT of the polymeric surfactant solution to be measured was introduced into a capillary tube and then closed with Teflon cap having a rubber spectrum. Then, a drop of the crude oil was injected into the tube through the rubber spectrum by using a syringe. Appropriate rotation speed was then adjusted, so that the crude oil droplet could be suitably elongated. Lastly, the IFT between the two fluids was calculated using built-in software in the system. IFT measurements were calibrated using Profile Fit measurement system (Laplace Transform, i.e., LY) by assessing the profile shape of the crude oil droplet in real-time mode. Indication of accuracy by using error function was calculated from Laplace (linear polynomial) fitting data in spinning drop experiments. Each experiment was repeated thrice and average IFT values are reported.

8. Rheological Studies

Rheological measurements involved a Bohlin Gemini 2 Rheometer (Malvern Instruments Ltd., UK), which is a model of an 'Advanced Air Bearing Rheometer'. The viscosity and shear rate measurements in viscometry mode were carried out using cup and bob (coaxial cylinder) measuring system. A small amount of the fluid was filled in a test cell referred to as the cup. A flat-faced bob was pressed into the cylindrical cup containing the fluid such that the vertical gap between the bob and the base of the cup containing the fluid is 0.5 μm. The bob in contact with the fluid in the cup was then rotated at varying specified speeds (strain rates). The force exerted by the fluid sample (in the narrow vertical gap between the bob and the base of the cup) on the cylinder was indicated by the value of the shear stress. The viscosity was measured by principle of drag created by the fluid on the cylindrical surface due to rotation of the bob. The range of shear rate for viscometry mode for this experiment varied from 1 to 1,000 s^{-1}, and the values of viscosity and shear stress were measured corresponding to the varying shear rates.

9. Contact Angle Measurement

The contact angle between synthesized polymeric surfactant solutions and sandstone surface were measured by contact angle goniometer (Drop shape Analyzer DSA25, Kruss, Germany) at 27 °C to evaluate wettability alteration. For, this, accurately measured 10 μL solution was carefully dropped on the top surface of the sandstone. Variations of contact angle with time were measured for wettability alteration study. Initially, the rock (sandstone) was made oil wet, keeping it inside the crude oil for aging. It was found that the rock was intermediate oil wet. Then the reduction of contact angle was measured putting the drop of surfactant on the oil wet sandstone surface and subsequent observation with time.

10. Flooding Experiments

Sandpack flood tests were employed for the evaluation of the effectiveness of the synthesized polymeric surfactant to enhanced oil recovery. A schematic of the experimental setup is reported in our earlier paper [24]. It consists of four components: a core holder, a displacement pump (Teledyne Isco), chemical solution cylinder and a fraction collector. As per homogeneous sand packing model, the geometry was chosen as L=43 cm and r=3 cm. The core holder was tightly packed with uniform sands (60-100 mesh) and saturated with 1.0 wt% brine. It was flooded with the brine at 25 psig and the absolute permeability was calculated from the flow rate and pressure drop through sand pack. The sand pack was then flooded

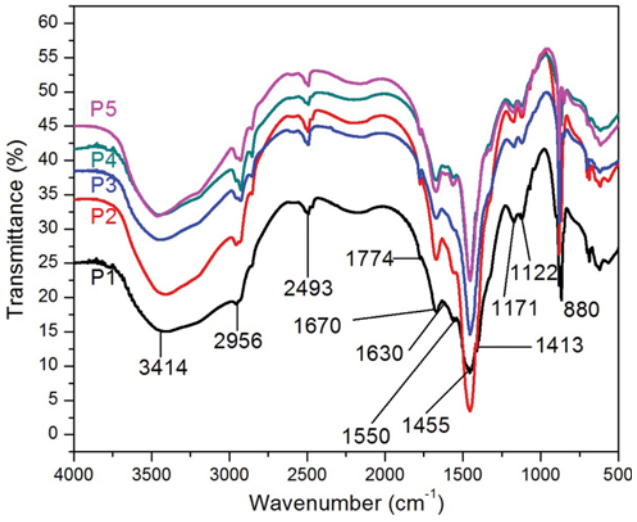

Fig. 2. FTIR spectrum of polymeric surfactants.

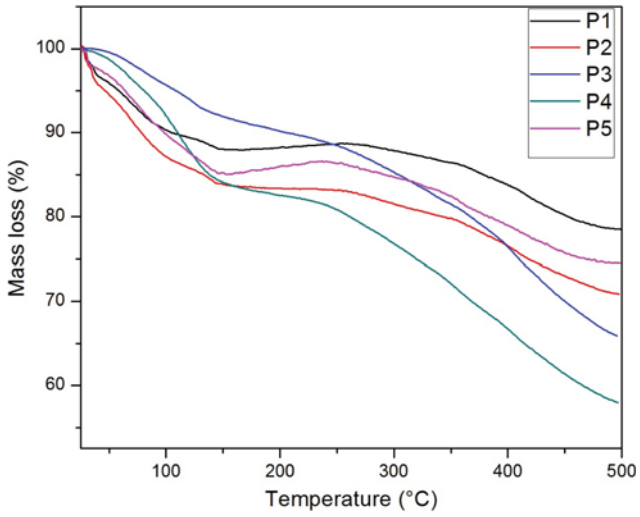

Fig. 3. Thermal stability curve for PMES surfactant.

with the crude oil at 800 psig to irreducible water saturation. The initial water saturation was determined on the basis of mass balance. The crude oil used in the flooding experiments was collected from Ahmedabad oil-field (India). The oil had a total acid number of 0.038 mg KOH/g, gravity of 38.86 °API and viscosity of 11.9 Pa·s at 30 °C. Water flooding was conducted by placing the core holder horizontally at a constant injection pressure at 200 pisg. After water flooding, when water-cut reached above 95%, around 0.5 pore volume (PV) of polymeric surfactant slug was injected followed by chase water flooding. The experiments were repeated using different concentrations of slug solutions. The additional recoveries were calculated by material balance.

RESULTS AND DISCUSSION

1. Measurement of FTIR

The infrared spectrum of different synthesised polymeric surfactants is illustrated in Fig. 2. The carbon-carbon double bond of polymeric surfactant was confirmed by the spectra at 1,670 cm^{-1}. Peak at 1,550 cm^{-1} shows the presence of N-H (amide group) due to the C=O stretching vibration. The tiny peaks from 3,414-2,956 cm^{-1} show the presence of primary and secondary amides due to N-H stretching. The peaks between 1,171-1,122 cm^{-1} and 1,413 cm^{-1} indicate the presence of sulfonate groups due to S=O stretching vibration. The absorbance peak at 1,774 cm^{-1} indicates the S=O stretching vibration indicating the presence of esters. The presence of the significant peak at 1,455 cm^{-1} corresponds to the asymmetrical bending vibration band of methyl group (C-H) [25]. The strong peaks at 1,413 cm^{-1} and 1,670 cm^{-1} represent the sulfonate and amide group stretching vibrations which show that this compound must be polymeric methyl ester sulfonate.

2. Thermal Analysis of Polymeric Surfactants

The thermal analysis of five different PMES samples was performed and is depicted in Fig. 3. Three mass loss steps were observed. The first thermal degradation that occurred at ambient to 100 °C is attributed to the loss of weakly bonded water molecules with an average of 8.4% mass loss. Then, an average of 12.89% mass loss occurred sharply in second region from 100 °C to 300 °C, revealing that PMES molecules start to decompose of amide group at temperatures exceeding 100 °C [26,27]. The third degradation region from 300 °C to 500 °C represents a complex thermal degradation, which may result from the condensation of the residual amide groups and cyclic amide rings. The degradation increases as surfactant-to-acrylamide ratio decreases. In P2, where the surfactant-to-acrylamide ratio is 1 : 0.5, TGA shows that the mass loss is minimum up to a moderate temperature (27 °C). It also shows the lowest interfacial tension of 6.54×10^{-2} mN/m and 2.0×10^{-3} mN/m for without NaCl and with NaCl, respectively. But as the usual reservoirs temperature ranges between 50 °C to 120 °C, the PMES surfactant retains an average of 94.91% of their original structure and mass [28]. It can be concluded that the PMES is thermally stable under the desired reservoir temperature.

3. Field Emission Scanning Electron Microscopy (FESEM) Analysis

The surface morphology of PMES surfactant observed by FESEM is shown in Fig. 4: the synthesized PMES surfactant has elongated spherical particle size with 1-5 μm in diameters and does not have a uniform size distribution. The particles of polymeric surfactant are in agglomerated form. The presence of elongated structure suggests that heating at higher temperature may lead to the formation of the elongated structure in PMES [29]. The results also proved completely that sodium chloride can destroy the molecular aggregation of polymeric surfactant. Because of interaction between sodium chloride and PMES, the molecular aggregation in solution is destroyed and the number of mono-molecules increases, which results reduction of IFT value by PMES solution in presence of sodium chloride [30].

4. Energy Dispersive X-Ray (EDX) Analysis of PMES Surfactant

Fig. 5 shows the EDX spectrum of PMES at various surfactant to acrylamide ratios. In the EDX spectrum, seven elements can be observed: carbon (C), sodium (Na), oxygen (O), nitrogen (N), gold (Au), chloride (Cl) and sulfur (S). The carbon is due to the organic intercalant in the PMES. The gold (Au) observed in the EDX is

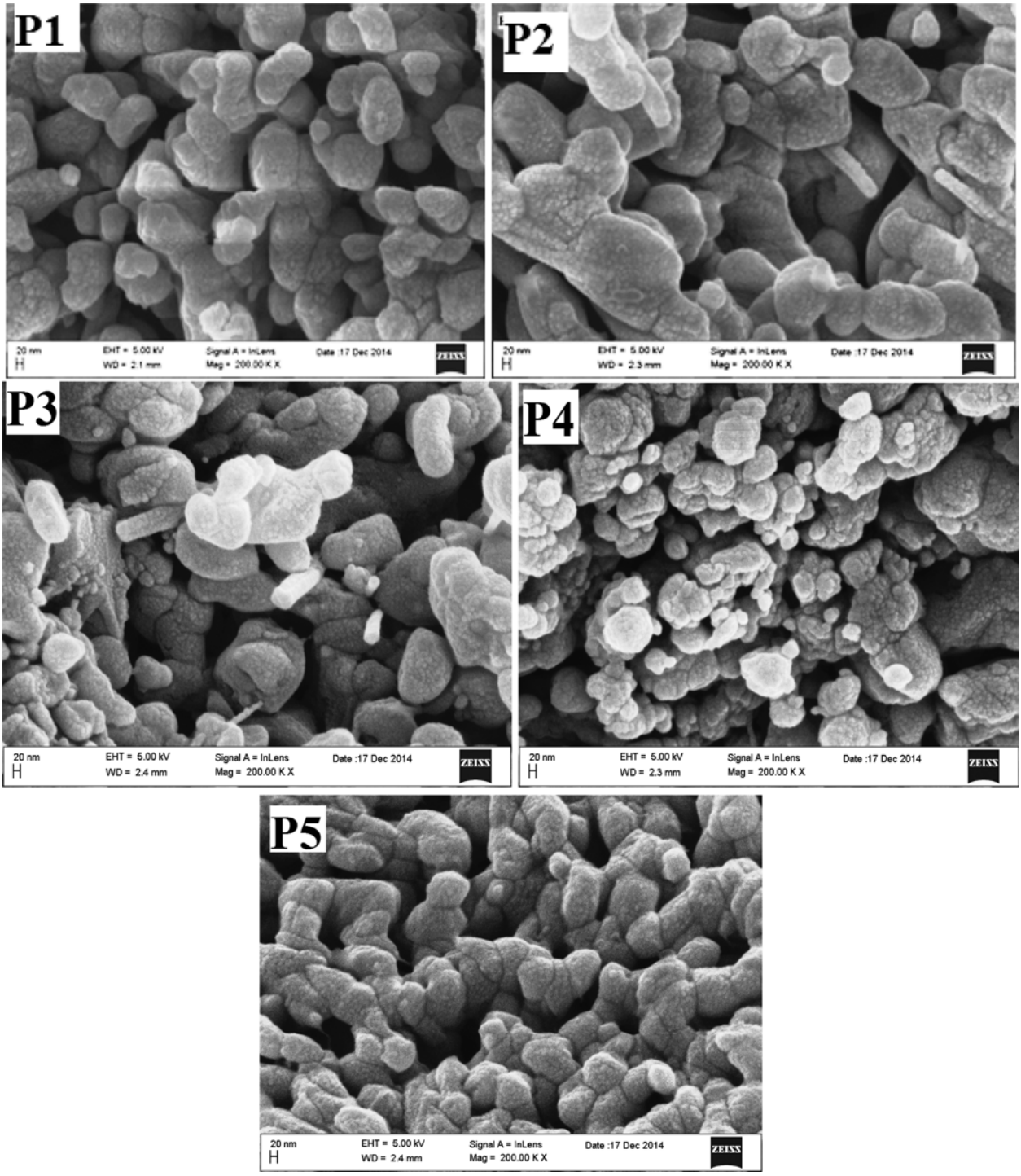

Fig. 4. FESEM image of PMES surfactant for different magnification: (P1) 20 nm (P2) 20 nm (P3) 20 nm (P4) 20 nm and (P5) 20 nm.

associated with the coating materials sputtered on the PMES. All remaining elements represent components of the polymeric surfactant. No other peak for any other element can be found in the spectrum, which confirms again that the polymeric surfactant is pure PMES [31].

5. Dynamic Light Scattering of Polymeric Surfactant Solutions

Fig. 6 shows that the hydrodynamic diameter increases with increasing the PMES surfactant concentration. It is understood that the increase of hydrodynamic diameter results from aggregation of the molecules. The movement of the particles gives rise to diffusion in various polymeric surfactant solutions, where the rate of diffusion is more rapid for small particles which means the particle size is small contributing to faster diffusion [32]. Thus, it may be concluded that with the increase in PMES surfactant concentration, the particle size increases simultaneously. The increase in higher hydrodynamic diameter of PMES with higher AMM: SEMS

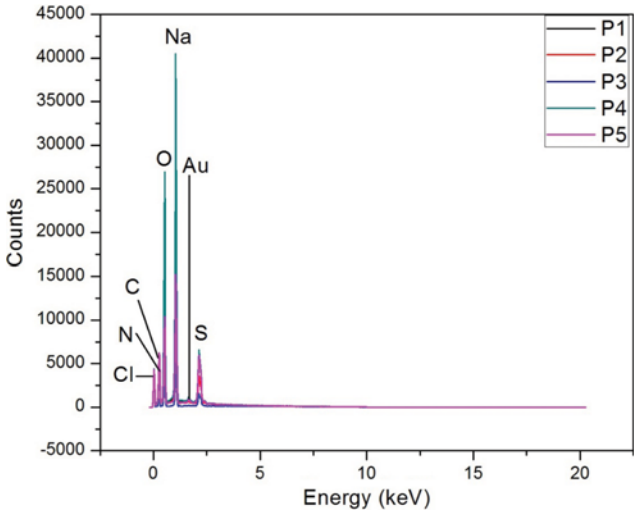

Fig. 5. EDX spectrum of polymeric surfactant.

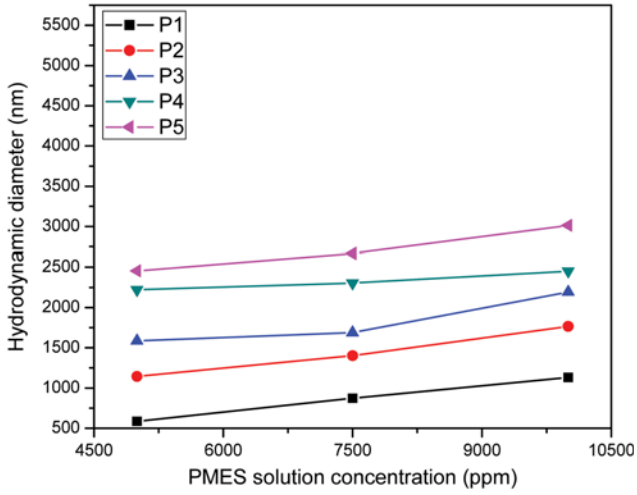

Fig. 6. Particle size analysis of different PMES surfactant solutions.

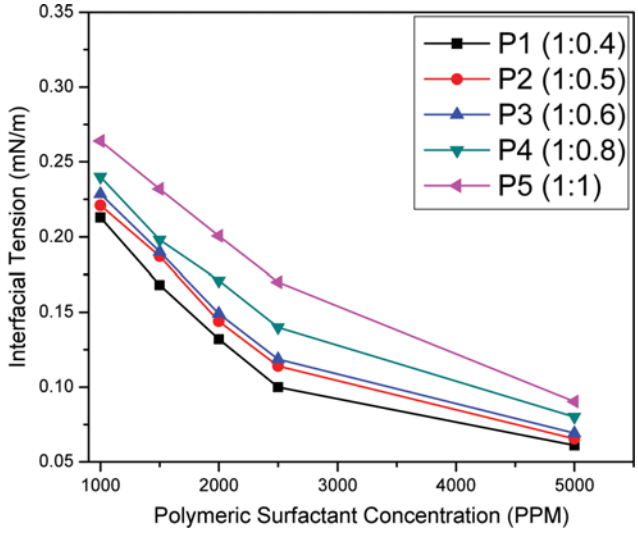

Fig. 7. Interfacial tension of polymeric surfactant at various concentrations.

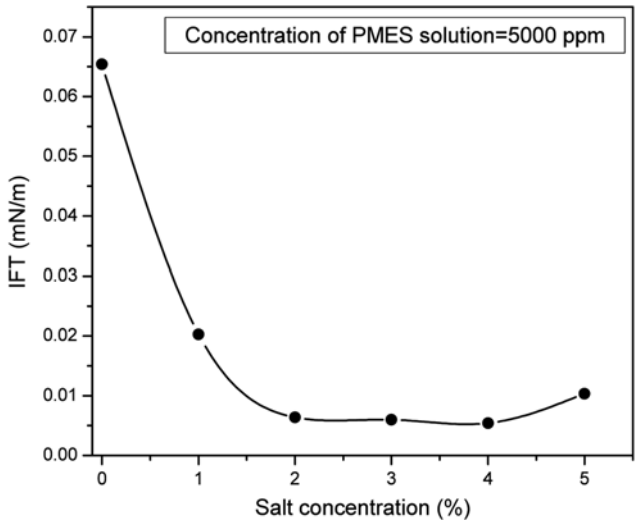

Fig. 8. IFT performance of PMES solution (P2) as a function of various salt concentrations.

ratio may be attributed to higher length of polymer chain of PMES.

6. Interfacial Tension (IFT) between Crude Oil and PMES Solutions

The interfacial tension of the polymeric surfactant was investigated using different weight ratios of surfactant to acrylamide as shown in Fig. 7. The IFT of a surfactant-crude oil system is greatly dependent on the adsorption of surfactant at the crude oil/water interface. Ultra-low values of IFT are obtained with synthesized PMES. This demonstrates the aggregative properties of the attached sulfonate group to the polymer chains. The figure shows the interfacial tension between crude oil and PMES solution decreases with increase in concentration of the PMES solutions. The ratio of SMES to AAM has significant effect on IFT in synthesized PMES. At higher AAM-to-SMES ratio the length of polymer chain increases, which causes increase in surface tension of PMES at a particular concentration.

7. Effect of Salt on IFT of PMES Solution

The effect of sodium chloride on the IFT performance of PMES solution of concentration 5,000 ppm is shown in Fig. 8. The IFT decreases significantly with the increase of sodium chloride concentration until it is 5.42×10^{-3} mN/m when the concentration of sodium chloride reaches 4 wt%. The sharp decrease of the IFT value in presence of salt can be explained by the fact the surfactant adsorbs more strongly at higher salt concentrations because it is less ionized. When a water soluble surfactant is less ionized, it becomes less water soluble and will adsorb more strongly at the interface. The natural surfactants are associated with the PMES to produce a synergistic effect. Thus, the concentration of 4 wt% sodium chloride is considered as the optimum salt concentration in P2 with surfactant to acrylamide ratio (1 : 0.5) [33].

8. Effect of Temperature on the Viscosity of PMES Solutions with Different Acrylamide-to-surfactant Ratios

The viscosity readings were carried out at 25 °C, 40 °C and 60 °C, and their varying effects were compared at a shear rate of 80 s^{-1} as shown in Fig. 9. The compositions of polymeric surfactant were taken at different weight ratios of SMES : AAM (1 : 0.4, 1 : 0.5, 1 : 0.6,

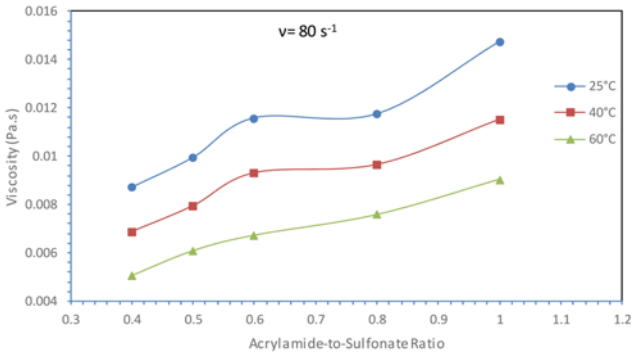

Fig. 9. Variation of dynamic viscosity of polymeric surfactant with Acrylamide-to-Sulfonate ratio of 2,500 ppm PMES Solution in distilled water at different temperatures.

1 : 0.8 and 1 : 1) at 2,500 ppm. The viscosity of polymeric surfactant is comparable to any polymer used for enhanced oil recovery. In the synthesized PMES as the acrylamide to sulfonate ratio increases, viscosity also increases because of increase in polymeric chain or increased molecular weight of the polymer. At all polymeric surfactant examined, the solution viscosity decreased with temperature. As temperature increased, the average speed of the molecules in a liquid increased and the time they spent in contact with their nearest neighbors decreased. Thus, as temperature increased, the average intermolecular forces decreased.

9. Wettability Alteration

Application of surfactants largely affects the wettability of solid surface, which is very important in the context of oil recovery, as the change of wettability of rock from oil wet to water wet increases the oil recovery. The interfacial crude oil-aqueous solution-solid substrate interactions are characterized by the formation of a contact angle on a solid surface. The knowledge of contact angle behavior is one of the challenging problems in surface science due to its role in all processes involved in three-phase interfacial phenomena. The contact angle is related to solid substrate structure and its surface roughness, whereas the second is associated with the mutual interactions of immiscible liquids in contact with the solid substrate. In the present study, the effect of polymeric surfactant was studied on sandstone. A schematic of contact angle between surfactant solution and initially oil wet rock at start and after 760 minutes is shown in Fig. 10. The change of contact angle versus time of rest on the initially oil wet sandstone surface for droplets PMES solution is reported in Fig. 11. The contact angle decreases initially sharply and then decreases slowly to a lower value, suggesting the potential effect of the PMES on wettability alteration from oil-wet to water-wet.

10. Oil Recovery by Flooding of Polymeric Surfactant (PMES) Solution

To determine the effects of polymeric surfactant concentration on the additional oil recovery, three sets of sandpack flooding (Sample S1, S2 and S3) were conducted using polymeric surfactant (P5) of different concentrations: 0.5, 0.6, and 0.7 mass%. The concentrations of the polymeric surfactant were kept above CMC considering the surfactant loss by adsorption during flooding. Polymeric surfactant slugs were injected when water cut reached ~95% during

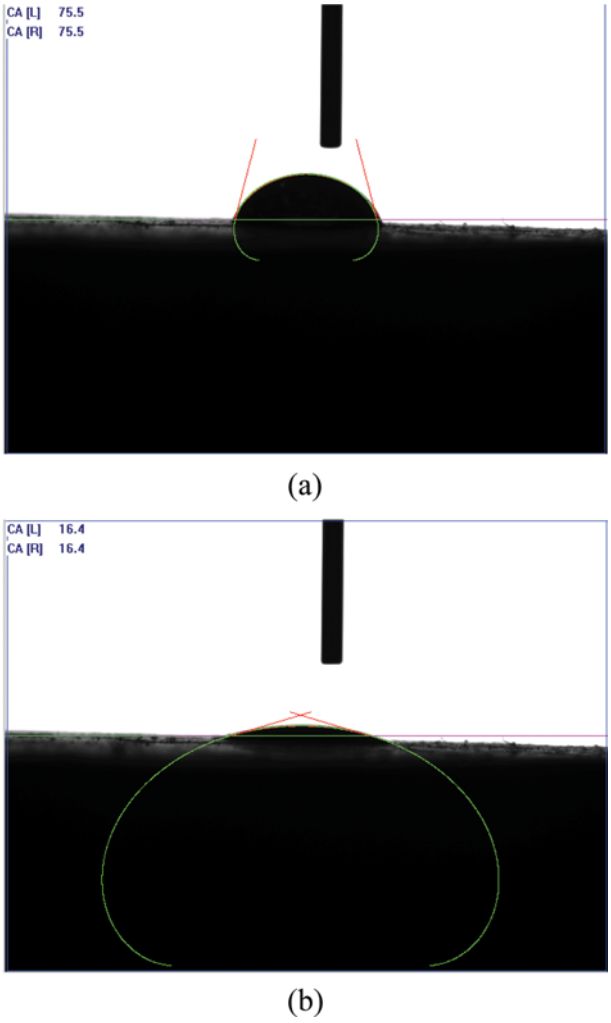

Fig. 10. Photographs of droplets of PMES solution (5,000 ppm) on sandstone surface (a) t=0 sec, (b) t=760 sec.

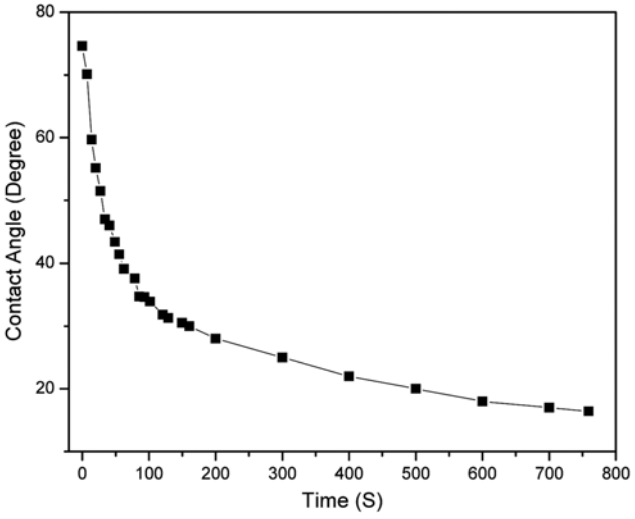

Fig. 11. Dynamic contact angles of droplets of PMES solution on sandstone at 25 °C.

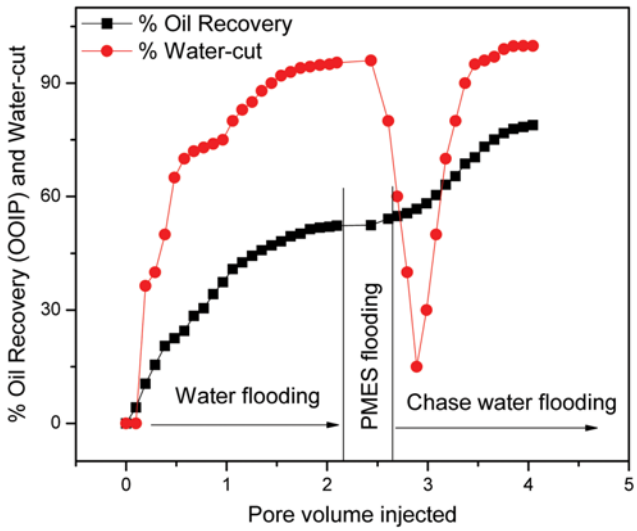

Fig. 12. Variation of oil recovery and water cut with injected pore volume for PMES (P5) flooding.

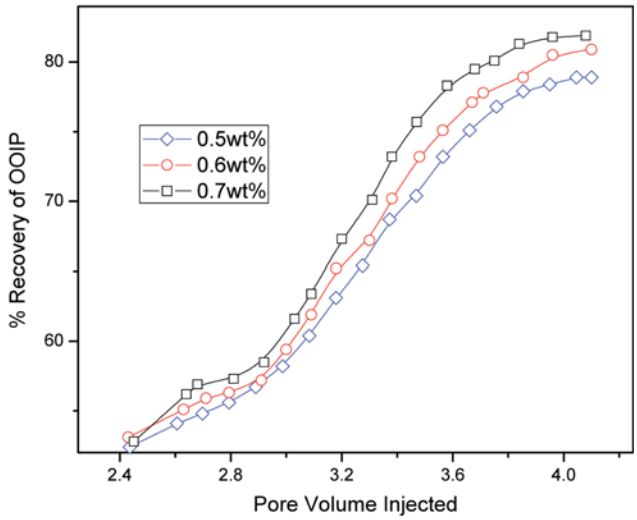

Fig. 13. Comparison of enhanced oil recovery of PMES (P5) flooding with three different concentrations.

water flooding. The oil recoveries and water-cut as function of pore volume injected of displacing fluids areen plotted in Fig. 12. Use of polymeric surfactant shows significant additional recovery after water flooding due to reduction of interfacial tension between oil, increase in mobility ratio and displacing fluid and consequent formation of oil bank. The additional recovery after the water flooding increases with increase in polymeric surfactant concentration. As the solution of polymeric surfactant was injected, a sudden drop in water-cut was observed due to decrease in relative permeability to water and water-cut then approached to 100% during chase water flooding. The effect of concentration of PMES on enhanced oil recovery is shown in Fig. 13. The additional recoveries over conventional water flooding along with other petrophysical properties are summarized in Table 1. The additional recoveries in polymeric surfactant flooding were found around 26.5%, 27.8% and 29.1% for 0.5, 0.6 and 0.7 mass% of polymeric surfactant solutions, respectively. Residual oil saturations were calculated by material balance equation.

CONCLUSION

Polymeric methyl ester sulfonate was synthesized from SMES for use as both surfactant and polymer in chemical enhanced oil recovery. FTIR spectrum data suggests the presence of sulfonate and amide group stretching vibration, which is evident from the strong peaks at 1,413 cm^{-1} and 1,670 cm^{-1}. This shows conclusive proof that this compound must be polymeric methyl ester sulfonate. The surface morphology of polymeric surfactant showing an elongated spherical shape suggests that heating at higher temperatures may lead to the formation of the elongated structure. Additionally, the polymeric methyl ester sulfonate showed a good thermal stability at reservoir temperature, where only 11.1% (average) mass loss is observed. The interfacial tension between crude oil and aqueous solutions of PMES and the viscosity of PMES solutions indicate it is an excellent chemical for chemical enhanced oil recovery. The presence of sodium chloride in PMES solution reduces the IFT to an ultra-low value (2.0×10^{-3} mN/m). Contact angle studies show that PMES solution has good potential on change of wettability from oil-wet to water-wet. Core flooding experiments show 26.5%, 27.8% and 29.1% additional recovery of crude oil for 0.5, 0.6 and 0.7 mass% of PMES surfactant solutions, respectively, after conventional water flooding. The synthesized polymeric surfactant is low cost for production and environment friendly, with outstanding potential for chemical enhanced oil recovery.

REFERENCES

1. A. Samanta, K. Ojha, A. Sarkar and A. Mandal, *Int. J. Oil Gas Coal Tech.*, **6**, 245 (2013).

Table 1. Recovery of oil by PMES (P5) surfactant flooding for three different systems

Sandpack sample No.	Porosity (%)	Permeability, k (Darcy)		Design of chemical slug for flooding	Recovery of oil after water flooding at 95% water cut (%OOIP)	Additional recovery (% OOIP)	% Saturation		
		k_w (S_w=1)	k_o (S_{wi})				S_{wi}	S_{oi}	S_{or}
S1	8.523	1.26	0.54	0.5 PV 0.5 mass% PMES+Chase water	52.4	26.5	21.68	78.32	15.92
S2	8.528	1.27	0.55	0.5 PV 0.6 mass% PMES+Chase water	53.1	27.8	21.19	78.81	15.05
S3	8.784	1.29	0.57	0.5 PV 0.7 mass% PMES+Chase water	52.8	29.1	21.00	79.00	14.30

2. B. S. Shiran and A. Skauge, *Energy Fuels*, **27**, 1223 (2013).
3. Z. Guo, M. Dong, Z. Chen and J. Yao, *Ind. Eng. Chem. Res.*, **52**, 911 (2013).
4. M. Ko, B. H. Chon, S. B. Jang and H. Y. Jang, *J. Ind. Eng. Chem.*, **20**, 228 (2014).
5. Y. Bai, C. Xiong, X. Shang and Y. Xin, *Energy Fuels*, **28**, 1829 (2014).
6. A. Bera, B. B. Guha and A. Mandal, *J. Chem. Eng. Data*, **59**, 89 (2014).
7. A. Bera, K. Ojha, T. Kumar and A. Mandal, *Energy Fuels*, **26**, 3634 (2012).
8. D. W. Green and G. P. Willhite, Enhanced Oil Recovery, SPE (1998).
9. S. Mishra, A. Bera and A. Mandal, *J. Pet. Eng.*, Article ID **395857**, 1 (2014).
10. R. N. Healy and R. L. Reed, *Soc. Pet. Eng. J.*, **14**, 491 (1974).
11. A. Samanta, K. Ojha, A. Sarkar and A. Mandal, *Adv. Petrol. Explor. Dev.*, **2**, 13 (2011).
12. K. A. Elraies, I. M. Tan, M. T. Fathaddin and A. Abo-Jabal, *Petrol. Sci. Technol.*, **29**, 1521 (2011).
13. Y. Cao and H. Li, *Eur. Polym. J.*, **38**, 1457 (2002).
14. S. Liu and S. P. Armes, *Curr. Opin. Colloid Interface Sci.*, **6**, 249 (2001).
15. L. Ye, R. Huang, J. Wu and H. Hoffmann, *Colloid. Polym. Sci.*, **282**, 305 (2004).
16. J. Xu, L. H. Shi and M. L. Ye, *J. Polym. Sci. Part B.*, **35**, 827 (1997).
17. K. A. Elraies, I. M. Tan, M. Awang and I. Saaid, *Petrol. Sci. Technol.*, **28**, 1799 (2010).
18. H. Jamshidi and A. Rabiee, *Adv. Mat. Sc. Eng.*, Article ID **728675**, 1 (2014).
19. R. Das, D. Das, P. Ghosh, A. Ghosh, S. Dhara, A. B. Panda and S. Pal, *Cellulose*, **22**, 313 (2015).
20. S. Pal, T. Nasim, A. Patra, S. Ghosh and A. B. Panda, *Int. J. Biological Macromolecules*, **47**, 623 (2010).
21. C. M. Setty, A. S. Deshmukh and A. M. Badiger, *Int. J. Biological Macromolecules*, **67**, 28 (2014).
22. B. S. Mitchell, An Introduction to Materials Engineering and Science for Chemical and Materials Engineers, Wiley, Hoboken, New Jersey (2004).
23. F. Rodriguez. Principle of Polymer Systems, 2nd Ed., McGraw-Hill (1982).
24. A. Bera, K. Ojha, T. Kumar and A. Mandal, *Fuel*, **121**, 198 (2014).
25. R. M. Silverstein, F. X. Webster and D. J. Kiemle, Spectrometric Identification of Organic Compounds, John Wiley & Sons, Inc. (2005).
26. S. Carlino, M. J. Hudson, *J. Solid State Ionics*, **110**, 153 (1998).
27. F. Prinetto, G. Ghiotti, P. Graffin and D. Tichit, *Micropor. Mesopor. Mater.*, **39**, 229 (2000).
28. L. S. Shi, *React. Func. Polym.*, **45**, 85 (2000).
29. A. Munin and F. Edwards-Lévy, *Pharmaceutics*, **3**, 793 (2011).
30. Y. Barakat, I. K. Basily, A. Mohammad and A. M. Youssef, *Brit. Polym. J.*, **21**, 459 (1989).
31. M. Alexandre and P. Dubois, *Mat. Sci. Eng. R.*, **28**, 1 (2000).
32. H. U. Kim and K. H. Lim, *Bull. Korean Chem. Soc.*, **25**, 382 (2004).
33. A. J. Prosser and E. I. Franses, *Colloids Surf., A: Physicochem. Eng. Aspects*, **178**, 1 (2001).